Flue Gas Cleaning With Alternative Processes and Reaction Media

Rasmussen, Søren Birk; Huang, Jun; Riisager, Anders; Hamma-Cugny, Hind; Rogez, Jacquez; Winnick, J.; Wassserscheid, Peter; Fehrmann, Rasmus

Published in:
E C S Transactions

Link to article, DOI:
10.1149/1.2798646

Publication date:
2007

Document Version
Publisher's PDF, also known as Version of record

ECS Transactions, 3 (35) 49-59 (2007)
10.1149/1.2798646, copyright The Electrochemical Society

Flue Gas Cleaning With Alternative Processes and Reaction Media

S. B. Rasmussen[a], J. Huang[a], A. Riisager[a], H. Hamma[a,b], J. Rogez[b], J. Winnick[c], P. Wasserscheid[d], and R. Fehrmann[a]

[a] Department of Chemistry and Center for Sustainable and Green Chemistry, Technical University of Denmark, DK-2800 Kgs. Lyngby, Denmark
[b] Laboratoire TECSEN, Faculté des Sciences et Techniques de St Jérôme, 13397 Marseille Cedex 20, France
[c] School of Chemical Engineering, Georgia Institute of Technology, GA 30332, USA
[d] Lehrstuhl für Chemische Reaktionstechnik, Universität Erlangen-Nürnberg, D-91058 Erlangen, Germany

Alternative methods to the traditional industrial NO_X and SO_X flue gas cleaning processes working at lower temperatures and/or leading to useful products are desired. In this work we present our latest results regarding the use of molten ionic media in electrocatalytic membrane separation, ionic liquid reversible absorption and supported ionic liquid deNO_X catalysis. Further development of the methods will hopefully make them suitable for installation in different positions in the flue gas duct as compared to the industrial methods available today.

Introduction

SO_2 emission is one of the most serious problems resulting from increased consumption of fossil fuels, as it contributes to formation of e.g. smog and acid rain which damages the environment. Up to now, flue-gas desulfurization (FGD) is one of the most effective techniques to control emission of SO_2 from combustion of fossil fuels like coal and petrol. A variety of the processes for SO_2 control, such as wet FGD, dry FGD, and semidry FGD processes, have been adopted widely in commercial units (1). However, the methods need a large amount of water and further treatment of the resultant wastewater, or produce by-products such as calcium sulfite. Compared to the conventional lime stone FGD process, the estimated operating costs of an electrochemical membrane process could become significantly lower. A membrane operating at a load of 250 A/m^2 with a polarization around 0.5-1.0 volt would operate at costs only 10-30% of the conventional process. Installation costs for the two processes are believed to be comparable. Apart from that, the electrochemical membrane process yields 100% pure sulfuric acid as a side product, which can be sold or easily reacted with lime stone to produce high quality gypsum.

A possible electrochemical cell for FGD consists of a fuel-cell type ceramic setup with the active electrolyte absorbed into the pores of the ceramic materials by capillary forces. Two porous LiNiO electrodes are separated by an inert porous YSZ matrix. The pore size distribution of the YSZ matrix must be around an order of magnitude lower than the electrodes, in order to ensure that it is 100% filled with electrolyte. The electrode has to be around 30% filled with electrolyte in order to optimize the interface regions between gas, liquid and solid phases. Figure 1 shows a principal drawing of this fuel-cell like system (2):

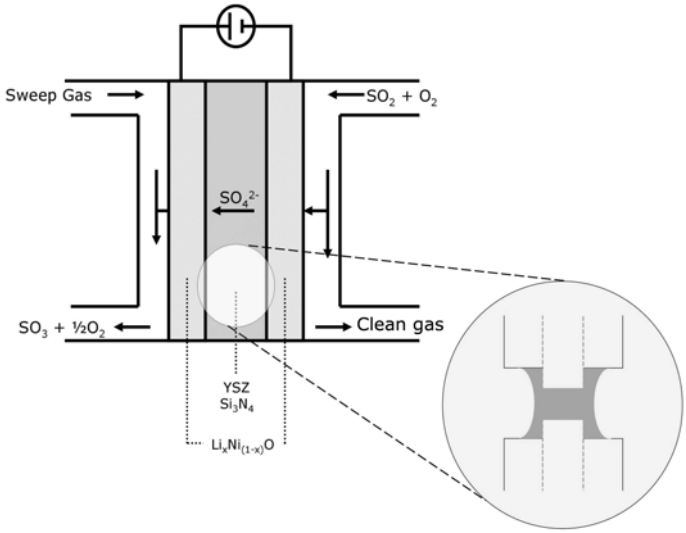

Figure 1: Principal drawing showing a fuel-cell like setup of the SO_2 removal cell. Insert represents schematically the ideal difference in pore size and capillary forces for the ceramic parts supporting the molten salt electrolyte.

The electrolyte is a molten salt based on an alkali/SO_4^{2-}/$S_2O_7^{2-}$ solvent with dissolved vanadium complexes. The salt is in molten form in the temperature range around 350-700°C, and the process is aimed to be working at 400°C. In such an electrochemical cell, the formal reactions during operation are:

Cathode: $$½O_2 + 2e^- \rightarrow O^{2-}$$ [1]

Electrolyte-cathodic interface: $$SO_3 + O^{2-} \rightarrow SO_4^{2-}$$ [2]

Anode: $$SO_4^{2-} \rightarrow SO_3 + ½O_2 + 2e^-$$ [3]

When V_2O_5 dissolves in a $M_2S_2O_7/M_2SO_4$ (M = Li, Na, K, Rb, Cs) molten salt, the following reaction occurs:

$$V_2O_5 + 2S_2O_7^{2-} \rightarrow (VO)_2O(SO_4)_4^{4-}$$ [4]

Depending of the activity of sulfate in the melt, more or less sulfate will coordinate with the dimeric complex, splitting it into two monomers:

$$(VO)_2O(SO_4)_4^{4-} + 2SO_4^{2-} \rightarrow 2VO_2(SO_4)_2^{3-} + S_2O_7^{2-}$$ [5]

Since these "side reactions" have influence on the performance of the cell an analysis of these melts are performed in this work.

Usually, the most attractive alternative approaches for SO_2 gas separation are pressure swing absorption (PSA) and temperature swing absorption (TSA) processes which are energy saving, by-product free, and the SO_2 can be used as excellent source for sulfuric acid production (3). Nevertheless, it is difficult to find an absorbent for reversible and selective absorption of SO_2. Generally liquid amines are used to chemically trap acidic gases such as, e.g. CO_2, SO_2, by formation of ammonium carbonate or sulfite. However,

in the case of large-scale SO_2 capture, the liquid amines can evaporate into the gas stream and the SO_2 is difficult to liberate from ammonium sulfite. Recently, Han and co-workers reported the use of an ionic liquid to reversibly absorb SO_2 (4).

Room-temperature ionic liquids (ILs) are attractive, environmentally acceptable solvents, as they combine very low vapor pressure and high thermal and chemical stability with excellent solvation ability for many organic and inorganic compounds. Therefore, they can also be used as environmentally benign solvents for a number of chemical processes such as separations (5) and reactions (6). Absorption of CO_2 using 1-*n*-propylamine-3-butylimidazolium tetrafluoroborate was studied by Bates et al. (7), and the results indicated that the IL can absorb CO_2 from gases effectively. In addition, it has been reported that ILs can dissolve many other gases, such as ethylene and ethane, especially at high pressure (8). Recently, we reported that several ILs are found to be excellent solvents for SO_2 by physical absorption of the gas (9). Here, we examine the application of ILs based on TMG (1,1,3,3-tetramethylguanidine) modified with alcohol groups originating from propylene oxide (PO) (Figure 2), for reversible and selective absorption of SO_2.

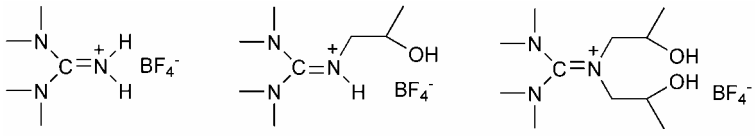

Figure 2: Ionic liquids of TMG and PO.

Also NO_X emissions are of increasing concern in the industrialized countries and stricter regulations of emission limits are envisaged. Emissions from fossil fueled power plants are usually reduced by installation in the gas duct of a V_2O_5/TiO_2 based heterogeneous catalyst converting NO_X to N_2 and H_2O by NH_3 injection in the flue gas. However, this SCR (Selective Catalytic Reduction) catalyst operates around 375°C and it has to be placed in a certain position in the flue gas duct. Thus a demand for flexible NO_X installations regarding temperature of operation and position in the duct will be needed. Also the increased use of biomass (straw, wood pellets etc.) alone or in combination with fossil fuel has been shown to decrease the life time of the V_2O_5/TiO_2 $deNO_X$ catalyst dramatically, due to deactivation by especially potassium salts in the biomass fly ash (10). Also for this reason alternative $deNO_X$ catalysts are demanded.

We are at present studying mechanisms of biomass deactivation of V_2O_5/TiO_2 catalysts and trying to develop other types of transition metal based heterogeneous $deNO_X$ catalysts (11). However, also other alternatives including $deNO_X$ active transition metal based ionic liquids are investigated by us. Here we report on the synthesis of a TiO_2 (anatase) supported ionic liquid doped with chromate, molybdate or tungstate complexes (TMG_2CrO_4, TMG_2MoO_4 and TMG_2WO_4) and on their activity as $deNO_X$ catalysts. High-valent chromium(VI), molybdenum(VI) and tungsten(VI) complexes with organic bases have previously been reported as effective and selective oxidants of primary and secondary alcohols in non-aqueous systems (12).

Experimental

Electrocatalytic membrane cell

Ceramics and housing. Stable, conductive $Li_XNi_{(1-X)}O$ electrodes were obtained by oxidizing Ni-mats from National Standard with 86% porosity to NiO by thermal treatment in air at 575°C overnight. Afterwards the material was soaked in aqueous LiOH and dried several times followed by another overnight thermal treatment at 575°C to insure intercalation of Li^+ into defects in the NiO structure. Finally the electrodes were washed, in order to remove excess Li^+, and then dried at 110°C. As porous, inert ceramic separators, yttria stabilized zirconia (Zircar 65%) were used. They had a thickness of 0.1 mm.

Molten salt electrolyte. The electrolyte was mixed from pure, dry potassium pyrosulfate, synthesized in the laboratory from $K_2S_2O_8$. $K_2S_2O_8$, V_2O_5, Cs_2SO_4, K_2SO_4, Li_2SO_4 and Na_2SO_4 were analytical grades from Merck. The electrolyte composition was found by a decanting procedure, which was chosen in order to obtain a mixture with high solubility of sulfate and vanadium, while still maintaining a reasonable good SO_2 oxidation catalytic activity. First the eutectic mixture of K_2SO_4 and V_2O_5 (40:60) % was mixed in the ratio 1:1 with the ternary sulfate $(Li, Na, K)_2SO_4$ eutectic and fused at 700°C. Hereafter, the melt was cooled to 510°C within 8 hours. Large parts of the salt had now solidified, but some remaining drops of liquid were decanted and analyzed. The resulting low melting sulfate-vanadia mixture was then mixed further with a $(K_2S_2O_7)_5V_2O_5$ salt, in order to obtain even lower temperature of fusion of the melt, and hereby at the same time ensuring a proper alkali metal composition with respect to catalytic capabilities. The final composition of this electrolyte candidate is $[(Li_{0.030}Na_{0.22}K_{0.55}Cs_{0.057})_2S_{3/2}O_{11/2}]_5V_2O_5$. The electrolyte was then used in full cell runs, incorporated into the separator YSZ-matrix..

Performance testing. Housings for bench scale testing of removal performance were made from machined 316S steel. The two identical housings that had 20 cm^2 circular wells for electrodes and gas channels to provide baffled gas flow to the electrode. The electronically conductive housings also served as current collectors. The pieces were assembled with electrodes in the wells and the ceramic matrix sandwiched between the two housings. The top housing had a drilled hole for optional use of a reference electrode and could also be used if electrolyte addition was necessary.

The assembled cell was placed in a brick furnace, and the temperature was controlled with a Barber-Coleman Model 122B controller connected to a double-pole solenoid which controlled the temperature within ±2°C. A PAR 173 potentiostat/galvanostat was used to control the current applied to the cell. Cell potentials were monitored both on the LCD display on the potentiostat/galvanostat and by Simpson 460 multi meters. Simulated flue gas with the composition 0.3% SO_2 and 5% O_2 in N_2 (Air-Gas) was fed to the compartment containing the cathode, while N_2 (Air Products) was fed to the anode side as purge gas. Analysis of SO_2 content was performed with a Perkin Elmer AutoSystem XL gas chromatograph, equipped with a Supelco 60/80 Chromosorb 102 2×1/8" column and a Flame Photometric Detector (FPD) which conveniently only monitored sulfur species, thus eliminating possible separation problems of effluents. SO_3 concentrations were determined by absorbing the effluent in de-ionized water followed by pH

measurements, following a procedure developed by Franke (13). Any positive error in reading due to partial absorption of SO_2 in the sample was regarded as insignificant.

Ionic liquid gas absorption

Ionic liquid synthesis. Lithium bis(trifluoromethanesulfonyl)amide, fluoroboric acid (50 wt% solution in water), 1,1,3,3-tetramethylguanidine (TMG), propyl bromide, and propylene oxide were purchased from Aldrich and SO_2 gas (99.95%) from Air Liquide. All reagents were used as received without any pretreatment.

The $[TMG][BF_4]$ (**1**) (Figure 2) ionic liquid was prepared directly by neutralization of TMG with fluoroboric acid (HBF_4) in ethanol solution (9,14). To an ice-bath cooled stirred solution of TMG (11.5 g, 0.10 mol) in ethanol (100 mL) concentrated fluoroboric acid (0.10 mol) was carefully added. *Caution: neutralization of base with a strong acid is highly exothermic.* Afterwards, the solvent was removed under reduced pressure with heating at 70°C followed by heating under high vacuum, yielding a colorless and viscous ionic liquid.

The ionic liquid $[TMGPO][BF_4]$ (**2**) was prepared by reacting propylene oxide with TMG (15). To a stirred solution of TMG (11.5 g, 0.10 mol) in toluene (100 mL) propylene oxide (0.10 mol) was added drop wise with stirring while maintaining the temperature at 20 °C. The reaction vessel was then sealed and stirred at room temperature for additionally 48 h. Afterwards, concentrated fluoroboric acid (0.10 mol) was carefully added to the stirred solution while cooling in an ice bath. After removal of the solvent under reduced pressure with heating at 70 °C and drying under high vacuum, a colorless and viscous ionic liquid was obtained.

$[TMGPO_2][BF_4]$ (**3**) was prepared by reaction of an additional equivalent of propylene oxide with $[TMGPO][BF_4]$, using a similar procedure as applied for the $[TMGPO][BF_4]$ synthesis above. In this way a colorless liquid was obtained which gradually became more viscous (without solidifying) upon extensive drying.

In all reactions the successful synthesis of the ionic liquids was confirmed by NMR spectroscopy.

Sulfur dioxide absorption. The absorption of SO_2 was carried out at ambient pressure (with pure SO_2) and at room temperature (20°C). The gas stream was bubbled through about 3.5 g of IL loaded into a glass tube with an inner diameter of 12 mm, and the flow rate was about 50 ml min^{-1}. The glass tube was partly immersed in an oil bath of which the temperature was controlled. The weight of the IL solution was determined at regular intervals. Desorption of SO_2 at various temperatures was also carried out with this glass tube in a temperature controlled oil bath. When SO_2 gas evolution ceased during desorption at the selected temperatures, the solution was weighted.

Ionic liquid deNO_X catalysts

Catalyst preparation. Firstly, aqueous solutions of TMG_2MO_4 (M = Cr, Mo or W) were prepared by directly mixing two mole equivalents of TMG with CrO_3, MoO_3 or WO_3 in water. After further addition of TiO_2 carrier, removal of water by evaporation and drying the supported catalysts were obtained.

In a typical catalyst synthesis, 1.0 mmol TMG (0.115 g) and 0.5 mmol metal oxide (0.050 g CrO_3, 0.072 g MoO_3 or 0.116 g WO_3) were added into 20 mL water to obtain solutions of TMG_2CrO_4, TMG_2MoO_4 or TMG_2WO_4, respectively. Anatase support (0.66

g, 0.74 g or 0.92 g, respectively) was added to the various solutions. After evaporation of the water and drying at 200ºC for 3 hours, catalysts with 20 wt% TMG_2MO_4 metal complex ionic liquid on anatase were applied for selective catalytic reducing (SCR) of NO by NH_3.

SCR deNO_X measurements. The catalytic activity measurements were performed at 1 bar with a conventional fixed-bed flow reactor containing the catalyst (0.060 g; 80 mesh) using the gases oxygen, ammonia and nitric oxide (all 1.0% in He). By premixing of the gases the inlet concentrations of NO and NH_3 to the reactor were adjusted to 1000 ppm whereas the O_2 concentration was adjusted to 5%. The total flow of the mixed inlet gas was maintained at 150 ml min^{-1}. The reaction temperature was measured by a calibrated thermocouple inserted directly into the catalyst bed. The reactants and products were analyzed on-line using a Jasco UV-Vis spectrometer equipped with a 10 cm gas cell.

Results and Discussion

Electrocatalytic membrane cell

The efficiency of the electrolytic mixture was tested in the bench scale electrochemical unit. This was done by measuring the SO_2 and SO_X (SO_2 + SO_3) levels from the outlet of the cathodic cell chamber. By adjusting the current applied to the cell, while observing the outlet levels, the efficiency of the cell as a function of current density can be measured. This is done by relating the molar amount of removed SO_2 compared to the molar amounts of electrons being pushed through the system by the current source:

$$N(SO_X) = i/2F \qquad [6]$$

$N(SO_X)$ is the flux of sulfur oxides originating from SO_2 that has been transported through the membrane. Figure 3 shows these efficiencies at three different temperatures.

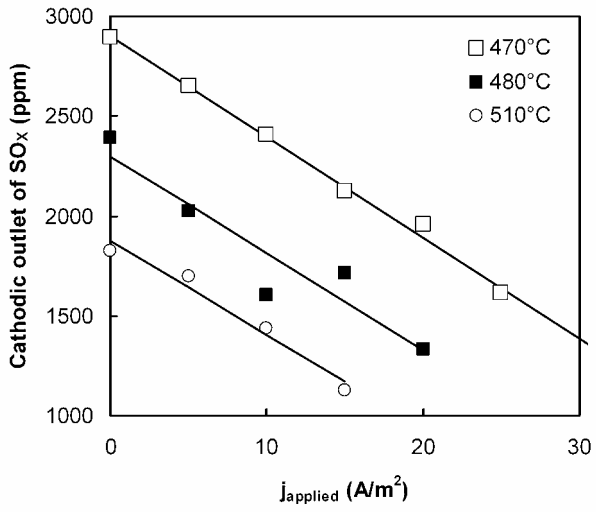

Figure 3: SO_X levels of emission from the cathodic chamber as a function of galvanostatic applied current in a 20 cm^2 bench scale full cell. The slopes correspond to a removal of 1 mol SO_2 per 2 electrons. The simulated flue gas is 2800 ppm SO_2, 4.8% O_2, 10% H_2O (balanced with N_2).

The slopes in Figure 3 correspond well to equation 6, which means that the current efficiency (or selectivity) at these temperatures is 100%. This is consistent with the overall scheme of reactions described by equation 1-3. A part from that, also zero current transport is ocurring, which can be seen by the deviation of the intercepts from the inlet concentration of 2800 ppm. This "free" transport is increasing with temperature. This can be explained by a set of chemical reactions starting from the cathode side, going towards the anode:

$$2SO_2 + O_2 \leftrightarrow 2SO_3 \quad [7]$$

$$SO_3 + 2V^{IV}O(SO_4)_3^{4-} \leftrightarrow SO_2 + 2V^{V}O_2(SO_4)_2^{3-} + S_2O_7^{2-} \quad [8]$$

$$SO_3 + 2V^{V}O_2(SO_4)_2^{3-} \leftrightarrow (V^{V}O)_2O(SO_4)_4^{4-} + SO_4^{2-} \quad [9]$$

$$SO_3 + SO_4^{2-} \leftrightarrow S_2O_7^{2-} \quad [10]$$

The equations 7-10 also occurs spontaneously, but reverse, on the anode side - especially if SO_3 continuously is removed due to a gas stream (sweep gas). This causes the equilibrium to be shifted towards the left. The rate of these reactions increase with the diffusivity of the sulfur species in the melt, and thus increases with temperature. The last point plotted for each temperature series (with highest current density), is the last point where 100% current efficiency was observed. At higher current densities there was a deviation from equation 6, and thus the mechanism given above is no longer followed. Even at 250 A/m^2 only around 30% removal was observed. Kinetic investigations showed that this was not because of limitations of the catalytically oxidation of SO_2. So there is a shift in the electrode process on the cathode side. This occurs more rapidly at high temperatures. This means that higher temperatures leads to higher activity but lower selectivity, and therefore the process has to run at moderate (400°C) temperatures. This is also more economical viable in an industrial application.

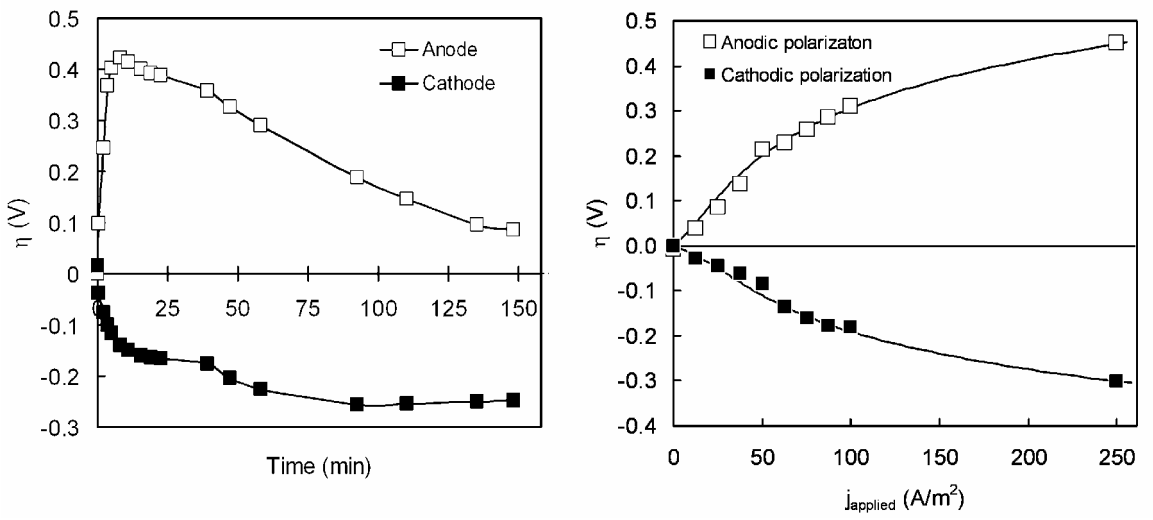

Figure 4: Polarization data from cell test.

Figure 4 shows the observed polarizations from the galvanostatic test at 470°C. To the right the anodic and cathodic polarizations as a function of current density are shown. If these polarizations are compared with previous tests done with conventional electrolytes significant improvements are achieved. This suggests that these new mixtures of salts make the electrolyte thermodynamically very stable, and they are less sensitive to

the occurring changes in the selectivity. In previous studies irreversible processes like crystallization of vanadium sulfate salts were observed. However, the above mentioned selectivity issues still leaves a challenge with respect to the capacity of the membrane process. The two parallel competitive reactions, mentioned above, can be explained by taking the complex chemistry of vanadium into account (16,17):

First a reduction of vanadium species:

$$2V^{V}O_2(SO_4)_2^{3-} + 2e^- + 2S_2O_7^{2-} \leftrightarrow 2V^{IV}O(SO_4)_3^{4-} + 2SO_4^{2-} \quad [11]$$

This is a likely key reaction, and is governed by the chemical environment near the cathode-electrolyte interface. If the cell works well, there will be sufficient SO_3 present to react with the formed vanadium complex:

$$SO_3 + 2V^{IV}O(SO_4)_3^{4-} \leftrightarrow SO_2 + 2V^{V}O_2(SO_4)_2^{3-} + S_2O_7^{2-} \quad [12]$$

The formed SO_2 is neutralized formally by the formation of two SO_3 molecules from SO_2 in equation 1. In this scenario, the sulfur oxide transport will then carry on by one of the following reactions:

$$2SO_4^{2-} \leftrightarrow 2SO_3 + O_2 + 4e^- \quad [13]$$

$$2S_2O_7^{2-} \leftrightarrow 4SO_3 + O_2 + 4e^- \quad [14]$$

$$2(VO)_2O(SO_4)_4^{4-} + 4SO_4^{2-} \leftrightarrow 4VO_2(SO_4)_2^{3-} + O_2 + 4SO_3 + 4e^- \quad [15]$$

$$2VO_2(SO_4)_2^{3-} \leftrightarrow 2VO_3^- + O_2 + 4SO_3 + 4e^- \quad [16]$$

These reactions follow two electron pathways. If a side reaction should occur, it can happen if the diffusion of SO_3 into the electrolyte is insufficient. At higher current densities the products from the cathodic electrode reaction doesn't react completely with SO_3. Instead some of the product migrates through the electrolyte and reacts as:

$$2SO_4^{2-} + 2V^{IV}O(SO_4)_3^{4-} \leftrightarrow 2V^{V}O_2(SO_4)_2^{3-} + 2S_2O_7^{2-} + 2e^- \quad [17]$$

which is the reverse of reaction in equation 11. This means that the applied electric field instead is used to move V(IV) and V(V) complexes back and forth without any useful transportation.

Figure 4 left shows the development of the polarizations over time, which support the explanation above. Immediately after the application of the electric field, the cathodic polarization is smaller than the anodic. This is because of the relative high activation polarization required to oxidize $S_2O_7^{2-}$. Since the V(IV) is formed by equation 11 near the cathode, it migrates towards the anode over time. The V(V)-V(IV) redox equilibrium have $E^0 \approx 0$ volt, and the result is an influence over time of the anode polarization due to the Nernst equation.

Ionic liquid gas absorption

The ionic liquids examined were found to absorb large amount of SO_2 gas corresponding to SO_2 to ILs molar ratios of 1.27, 1.62, 2.01 (wt %: 40.1%, 39.7%, 40.2%) for [TMG][BF_4], [TMGPO][BF_4] and [$TMGPO_2$][BF_4], respectively, after saturation with SO_2 gas at 1 bar and 20 ºC. Desorption of the absorbed SO_2 was carried

out by heating the saturated ILs while monitoring the weight loss periodically. In Figure 5 the SO_2 content in the ILs (as molar ratio of SO_2 to IL) as function of desorption temperature is shown. For all the ILs examined the SO_2 gas can be desorbed almost completely when heated to about 140 ºC.

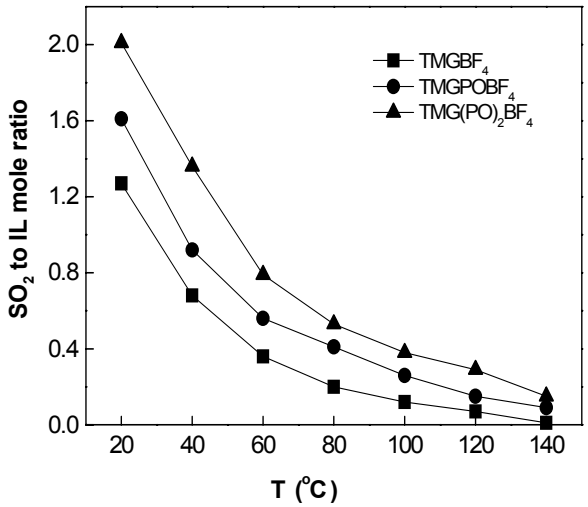

Figure 5: Desorption by heating shown as SO_2 to IL mole ratio against temperature.

Both absorption and desorption of SO_2 gas in the three examined ILs were relatively fast, providing complete absorption in one hour with pure SO_2 gas (50 ml min^{-1}, 200 rpm stirring), and most complete gas desorption in half an hour at room-temperature and 20Pa vacuum. Moreover, the ILs could be reused many times without any loss of absorption capability. In Figure 6 six consecutive absorption cycles are shown.

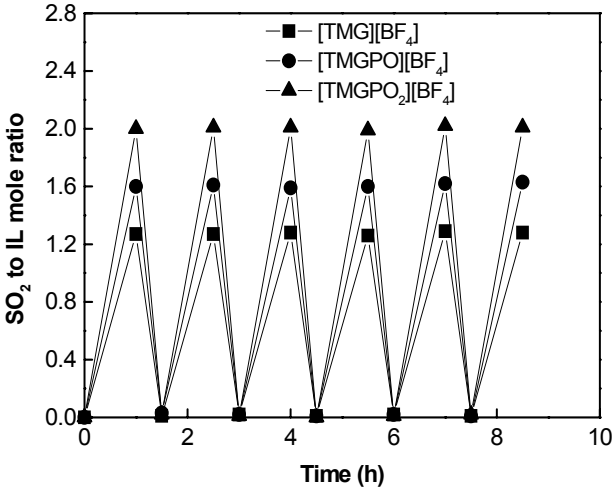

Figure 6: Repeated absorption and desorption of SO_2 by the ILs vs. time.

When 10% SO_2 gas (10% mole percent in N_2) was absorbed at ambient pressure in the ILs instead of pure SO_2 in order to simulate flue gas removal, SO_2 to IL molar ratios of 0.064, 0.151 and 0.201 were obtained at equilibrium for $[TMG][BF_4]$, $[TMGPO][BF_4]$ and $[TMGPO_2][BF_4]$, respectively. These values corresponds to an approximately ten-

fold decrease in absorption capacities when reducing the SO_2 partial pressure from 1 bar to 0.1 bar (as also expected from Raoult's law), allowing an estimated gas-liquid molar concentration ratio of 1:200 to be determined. The relatively higher absorption capability of the ILs $[TMGPO][BF_4]$ and $[TMGPO_2][BF_4]$ compared to $[TMG][BF_4]$ probably relates to an increased strength of the electrostatic force between the IL cation and SO_2 gas facilitated by the presence of OH groups.

Ionic liquid $deNO_X$ catalysts

The prepared metal oxide ionic liquid catalyst were tested for SCR $deNO_X$ activity in simulated flue gas as shown in Figure 7. The relative activity of the group 6 transition metal catalysts decrease in the order Cr > Mo > W, where tungsten exhibited a very low activity in the measured temperature range. Compared to the industrial vanadium oxide based catalyst the Cr based catalyst produced similar conversion efficiencies at much lower operating temperatures, possibly making the catalyst a viable alternative to present commercial $deNO_X$ catalysts. The stability of the metal oxide ionic liquid might, however, limit the useful temperature range for the catalyst compared to the heterogeneous industrial V_2O_5/TiO_2 catalyst which presumably is more active above, e.g. 300°C. Whether the metal oxide ionic liquid catalyst under working conditions is homogeneous is subject of ongoing investigations as is further optimization of the carrier material and loading with the active metal oxide ionic liquid.

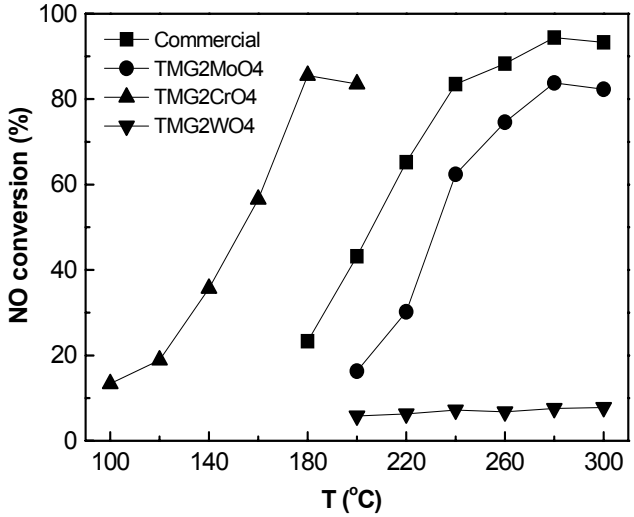

Figure 7: NO conversion of 0.060 g of the indicated metal oxide ionic liquid catalyst (20% w/w on TiO_2). Results for an industrial $deNO_X$ catalyst are given for comparison. Gas composition: 1000 ppm NO, 1000 ppm NH_3, 5% O_2, balance He. Total flow rate 150 ml min^{-1}.

Perspectives

The methods presented here are promising as alternatives to the traditional industrial $deSO_X$ and $deNO_X$ processes. Regarding the electrocatalytic membrane and the ionic liquid absorption processes a useful product, sulfuric acid, is obtained instead of waste or gypsum produced by most existing flue gas cleaning methods. With respect to catalytic

NO_X removal the results show that it might be possible to develop an alternative deNO_X catalyst working at lower temperature than the industrial catalyst used today. Possible also an ionic liquid suitable for selective reversible absorption of NO might be developed as shown here for SO_2. All of these alternative methods may lead to the desired flexibility regarding their positioning in the flue gas duct in, e.g. power plants. These methods are also envisaged to be less or non-sensitive to, e.g. potassium salts in the flue gas from biomass fired plants.

Acknowledgements

Support of the work by the Danish Research Council for Technology and Production, the Lundbeck Foundation and Elkraft Systems (PSO FU5201) are gratefully acknowledged.

References

1. X. Ma, T. Kaneko, T. Tashimo, T. Yoshida and K. Kato, *Chem. Eng. Sci.* **49**, 4643 (2000).
2. S. B. Rasmussen, K. M. Eriksen, R. Fehrmann and J. Winnick, *J. Appl. Electrochem*., **32**, 19 (2002).
3. S. M. Jeong and S. D. Kim, *Ind. Eng. Chem. Res.*, **39**, 1911 (2000).
4. W. Wu, B. Han, H. Gao, Z. Liu, T. Jiang and J. Huang, *Angew. Chem. Int. Ed.*, **43**, 2415 (2004).
5. a) P. Wasserscheid and W. Keim, *Angew. Chem. Int. Ed. Engl.*, **39**, 3772 (2000); b) T. Welton, *Chem. Rev.*, **99**, 2071 (1999); c) A. Bosmann, G. Francio, E. Janssen, M. Solinas, W. Leitner and P. Wasserscheid, *Angew. Chem. Int. Ed. Engl.*, **40**, 2697 (2001); d) J. Dupont, R. F. Souza and P. A. Z. Suarez, *Chem. Rev.*, **102**, 3667 (2002).
6. A. Riisager, R. Fehrmann, S. Flicker, R. van Hal, M. Haumann and P. Wasserscheid, *Angew. Chem. Int. Ed.*, **44**, 815 (2005).
7. E. D. Bates, R. D. Mayton, I. Ntai and J. H. Davis, Jr., *J. Am. Chem. Soc.*, **124**, 926 (2002).
8. J. L. Anthony, E. J. Maginn and J. F. Brennecke, *J. Phys. Chem. B*, **106**, 7315 (2002).
9. J. Huang, A. Riisager, P. Wasserscheid and R. Fehrmann, *Chem. Commun.*, 4027 (2006).
10. J. Chen and R. Yang, *J. Catal.*, **125**, 411 (1990).
11. A. L. Kustov, M. Kustova, R. Fehrmann and P. Simonsen, *Appl. Catal. B*, **58**, 97 (2005).
12. T. Waters, R. A. J. O'Hair and A. G. Wedd, *J. Am. Chem. Soc*., **125**, 3384 (2003).
13. M. Franke and J. Winnick, *Ind. Eng. Chem. Res.*, **28**, 1352 (1989).
14. J. Huang, T. Jiang, H. Gao, B. Han, Z. Liu, W. Wu, Y. Chang and G. Zhao, *Angew. Chem. Int. Ed.*, **43**, 1397 (2004).
15. J. D. Holbrey, M. B. Turner, W. M. Reichert and R. D. Rogers, *Green Chem.*, **5**, 731 (2003).
16. S. B. Rasmussen, K. M. Eriksen and R. Fehrmann, *J. Phys. Chem.*, **103**, 145 (1999).
17. O. B. Lapina, B. S. Bal'zhimaev, S. Boghosian, K. M. Eriksen and R. Fehrmann, *Catal. Today*, **51**, 469 (1999).